

# We are IntechOpen, the world's leading publisher of Open Access books Built by scientists, for scientists

## 4,800

Open access books available

## 122,000

International authors and editors

## 135M

Downloads

Our authors are among the

## 154

Countries delivered to

## TOP 1%

most cited scientists

## 12.2%

Contributors from top 500 universities

**WEB OF SCIENCE™**Selection of our books indexed in the Book Citation Index  
in Web of Science™ Core Collection (BKCI)

Interested in publishing with us?  
Contact [book.department@intechopen.com](mailto:book.department@intechopen.com)

Numbers displayed above are based on latest data collected.

For more information visit [www.intechopen.com](http://www.intechopen.com)

# Finite Element Modelling of Micro-cantilevers Used as Chemical Sensors

G. Louarn and S. Cuenot  
*Institut des Matériaux Jean Rouxel, University of Nantes  
France*

## 1. Introduction

During the last twenty years, the spectacular advances in micro-mechanical systems, and more generally in micro-electro-mechanical systems (MEMS), have enabled the emergence of an innovative family of biological and chemical sensors. The functionality of such sensors involved the transduction of a mechanical energy, which comes from the deformations of the micro-machined components. Among the different geometrical shapes of these components, clamped-free beams also called cantilevers represent the simplest MEMS. Although cantilevers play a role of basic building block for complex MEMS devices, they are nowadays widely used as force sensor probes in atomic force microscopy (AFM).

The recent developments of AFM have enabled the mass-fabrication of micrometer-sized cantilevers with various geometrical shapes and different materials (silicon, silicon nitride...) (). Indeed, beam cantilevers but also V-shaped cantilevers are commercially available with different dimensions. Recently, this variety of AFM cantilevers is become the base of a novel class of highly sensitive sensors operating essentially for chemical and biological detections (Raiteri et al., 2001 ; Sepaniak et al., 2002 ; Moulin et al., 2003 ; Lavrik et al., 2004). These micro-cantilevers, which can be extremely versatile sensors, present many advantages such as a relatively low cost of production and a reduced size of the active area (typically  $10^{-6}$  cm<sup>2</sup>). The detection principle of such sensors is based on the measurement of the cantilever deflection change or of the resonance frequency change of the cantilever (figure 1). These changes are induced by the adsorption of chemical species on the functionalized surface of a micro-cantilever (Chen et al., 1995 ; Betts et al., 2000).

Such adsorption may come from the interactions between specific molecules present in analyte and the sensitive coating of the cantilever. The measurement of the resonance frequency shift offers the interesting advantage to be relatively insensitive to interference from external factors such as thermal drift. Therefore, this method seems particularly well-suited for use in various environments such as gaseous or vacuum ones, and to measure the cantilever response upon exposure to optical radiation and to chemical vapours. Several applications of these AFM micro-cantilevers as sensors were developed during the ten last years (Lange et al., 2002 ; Baselt et al., 2003). According to the realized coating, the chemically modified surfaces of cantilevers can be used to produce transducers that are activated for specific analytes. For instance, cantilevers coated with a thin gold film become ideal sensors to achieve ultrasensitive detection of mercury vapour (Thundat et al., 1995a). A

metallic coating allows the calorimetric detection of chemical reactions with picojoule sensitivity (Gimzewski et al., 1994), while a gelatine coating is sensitive to the changes in relative humidity (Wachter & Thundat et al., 1995). Others detection can also be achieved such as pH-variation (Ji et al., 2001 ; Bashir et al., 2002) or optical radiation by coating the cantilevers with ultraviolet cross-linking polymers (Thundat, 1995b).

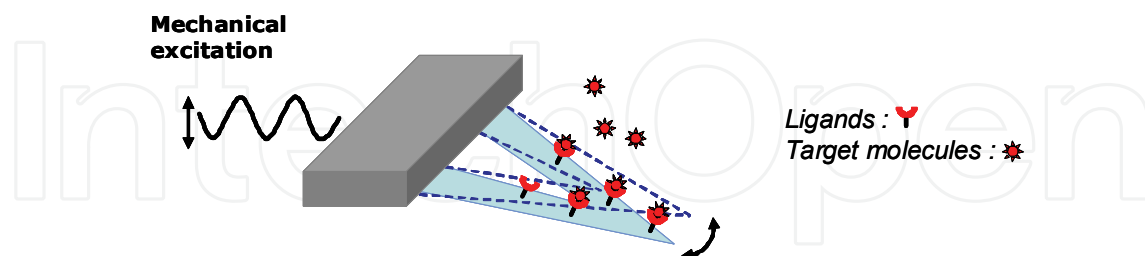


Figure 1. Cantilever deflection change induced by the adsorption of chemical species on the functionalized surface

In order to predict the sensitivity of these versatile sensors, it is crucial to precisely calculate the resonance frequencies of these micro-cantilevers (Dufour et al., 2003 ; Lochan et al., 2005). The resonance frequencies can be only calculated analytically for cantilevers with simple geometries like straight beams. In the other cases, for multilayer structures or more complex shapes, where the cross-section is not constant along the cantilever length (case of “V-shaped” micro-cantilevers), the resonance frequencies can not be analytically calculated. Among the different approaches allowing to calculate them, the finite element modelling (FEM) seems to be a particularly interesting approach. In this chapter, FEM is applied to “V-shaped” silicon micro-cantilevers for predicting their resonance frequencies and the sensitivity of these cantilevers employed as chemical sensors.

First, in order to validate the accuracy of the FEM approach, we carried out a comparison between analytical, experimental and FEM-computed values of the resonance frequencies for homogenous rectangular shaped micro-cantilevers. Then, we performed a modelling of silicon beams coated with a thin metallic layer. To precisely calculate the resonance frequencies of these multilayer-cantilevers, the influence of the mesh parameters on the calculated frequencies was strongly investigated.

Second, the sensitivity of different “V-shaped” silicon cantilevers was estimated, as a function of their geometrical dimensions and of their mechanical parameters (Young modulus, density). The resonance frequencies of uncoated cantilevers were calculated and compared with the values experimentally determined. Then, a similar approach could be employed to predict the sensitivities of such cantilevers recovered with a sensitive layer.

This chapter clearly shows that the use of finite element modelling allows the computation of the resonance frequencies of micro-sized cantilevers having a complex shape. Moreover, in the case of applications as sensors based on the resonance frequency measurement, this approach offers the ability to predict the sensitivity of multilayer-cantilevers. In this way, by simple calculation, the shape and the geometrical dimensions of these cantilevers can be optimized for obtaining the best sensitivities and detection limits.

## 2. Natural frequencies and normal modes of vibration

When a linear mechanical system undergoes free vibrations, i.e. without being subjected to any external periodic load, its behaviour is characterized by its so-called “eigen modes”. An

eigen mode is a global synchronous type of motion where the various degrees of freedom exhibit all the same time behaviour (with different amplitudes), viz. harmonic motion at a frequency which is characteristic of the mode. An  $n$  degrees of freedom system has  $n$  eigen modes, hence  $n$  characteristic eigen frequencies, also called “natural” frequencies.

When the system undergoes forced harmonic vibration, its behaviour is characterized by the frequency response relating the amplitude (and phase) of the steady-state harmonic response to that of the excitation. The main feature of this response is a series of peaks appearing at forcing frequencies close to the natural frequencies. These large response amplitudes (theoretically infinite if no damping is present) relate to the so-called “resonant” behaviour of the system – generally to be avoided in practice in most engineering application.

When the system is undamped, the (infinite) resonance peaks appear at forcing frequencies, which are identical to the natural frequencies of the system. From a physical point of view, since the system is excited at a frequency at which it would tend to freely oscillate, its vibration amplitude increases steadily, tending towards infinity.

In the case of a damped system, there are various definitions of the related “resonance” frequencies. One of these is the forcing frequency (close to a natural frequency) at which the maximum of a peak is reached. However, at a forcing frequency equal to a natural frequency, the phase shift between the response and the excitation is always an odd multiple of  $90^\circ$ , and this is generally chosen as the most reliable and accurate definition of resonance.

We see therefore that “natural” and “resonance” frequencies are two names for the same notion, albeit related to two different situations (“free” and “forced” vibrations). In the following, we shall use the term “natural” frequencies when analyzing free vibrations, and “resonance” frequencies when dealing with forced vibrations.

### 3. Experimental procedure

Nowadays, the atomic force microscopy (AFM) is widely used to characterize the surface of all kinds of materials, conductive as well as insulating samples. Although the most innovative advent of the AFM is its ability to measure locally different physical properties, the AFM offers real tri-dimensional images of the sample surface (Cuenot, et al., 2003).

The sample is fixed onto a piezoelectric ceramic, which has the property to expand or to contract when a voltage is applied. By scanning across the surface with an AFM tip, topographical information can be easily obtained from atomic-scale imaging to micron-sized images. In contact mode, topographic images can be achieved by two ways. First, by measuring directly the vertical deflection of the cantilever, which indicates the local sample height, when the AFM tip scans the sample. To measure this vertical deflection, a laser beam focused on the gold coating of the cantilever backside is reflected onto a photo-detector consisting of two side-by-side photodiodes. The difference between the signals coming from the up-and-down photodiodes reflects the vertical deflection of the cantilever (figure 2).

Second, topographic images can also be obtained by recording the vertical displacement of the piezoelectric ceramic when a constant force is applied by the tip on the sample surface. Indeed, the feedback loop existing between the ceramic and the photodiodes allows to keep the same cantilever deflection (i.e. a constant value of tension read from the photodiodes) by varying the voltage applied to the ceramic and hence adjusts the height of the sample.

In this chapter, the resonance frequencies of different cantilevers were measured. To measure them, a piezoelectric bimorph (located under the cantilever) is used to induce the

cantilever oscillations. By monitoring the cantilever deflection signal as a function of the frequency sweep of the bimorph, it is possible to completely characterize the resonance spectrum of cantilever.

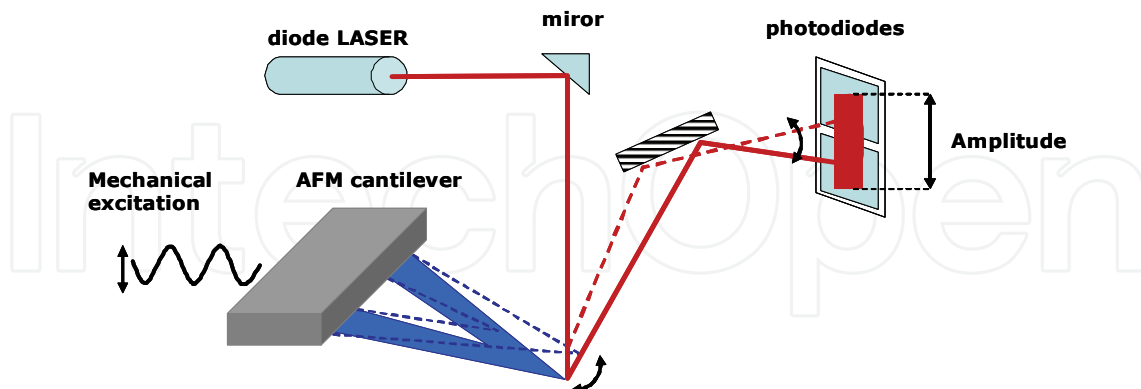


Figure 2. Principle of detection of the AFM

#### 4. Natural frequencies of free rectangular cantilevers

The fundamental vibration mode of a cantilever, i.e. the one with the lowest resonance frequency, always corresponds to a flexural vibration mode. The natural frequencies related to this vibration mode will be computed in the following sections.

##### 4.1 Analytical calculation

For many practical applications, the natural frequencies of uniform beam can be determined with sufficient accuracy by an analytical approach (Stokey, 1988). The classical approach is based on the use of the relation which relates the curvature of the beam to the bending moment at each section of the beam :

$$M = EI\chi = EI \frac{\partial^2 y}{\partial x^2} \quad (1)$$

This equation is based upon the assumptions that the material is homogeneous, isotropic and obeys Hooke's law. The beam must be straight with a uniform cross section. In order to neglect the shear deflection, the lateral displacement in direction of the  $y$  axis,  $y(x,t)$ , has to be small and the beam has to be long compared to cross sectional dimensions.

$E$  is the modulus of elasticity in tension and compression (Young's modulus), and  $I$  is the area moment of inertia.

The equation of motion for lateral vibration is found by considering the force action on the element which is formed by passing two parallel planes A and B through the beam normal to the longitudinal axis (figure 3). The vertical elastic shear force acting on section A and B are  $V$  and  $V' = V + (\partial V / \partial x) dx$  respectively (figure 3). The sum of the vertical forces acting on the element must equal the product of the mass of the element and the acceleration ( $\partial^2 y / \partial t^2$ ) in the lateral direction:

$$\frac{\partial V}{\partial x} + \rho S \frac{\partial^2 y}{\partial t^2} = 0 \quad (2)$$

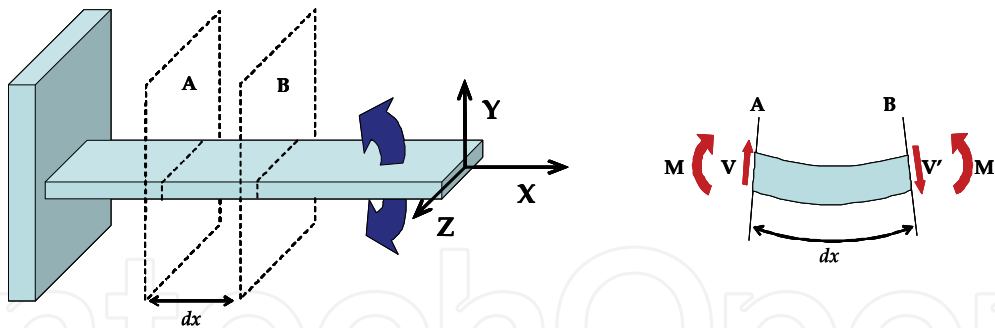


Figure 3. clamped-free beam executing lateral vibration, (B) element of beam showing shear force and bending moments

In this element, the equilibrium of the moment drives to  $V = \partial M / \partial x$ . Other differentials of higher order can be neglected. Then, from eq. 1 and 2, the basic equation for the lateral vibration of beams is given :

$$\frac{\partial^2}{\partial x^2} \left( EI \frac{\partial^2 y}{\partial x^2} \right) + \rho S \frac{\partial^2 y}{\partial t^2} = 0 \quad (3)$$

The solution of this equation if  $EI$  is constant, is of the form  $y = A(x) \times [\cos(\omega_n t + \varphi)]$  in which  $A$  is a function of  $x$  only. Substituting  $\beta^4 = \rho S \omega^2 / EI$  and dividing eq (3) by  $\cos(\omega_n t + \varphi)$  :

$$\frac{d^4 A(x)}{dx^4} = \beta^4 A(x) \quad (4)$$

The following function represents the solution of the eq. (4). The constants  $A, B, C, D$  are found from the boundary conditions.

$$A(x) = A \operatorname{ch} \beta x + B \operatorname{sh} \beta x + C \cos \beta x + D \sin \beta x \quad (5)$$

In applying the end conditions in the case of a rectangular beam, clamped at one extremity and free at the other, we have to solve the following equation:

$$1 + \operatorname{ch} \beta \ell \cos \beta \ell = 0 \quad (6)$$

With  $\ell$  the length of the beam. The solutions of that transcendental equation can be estimated from a numerical approach. As an example, with the Newton's method implemented with Matlab2007, we are able to found  $\lambda_n = \beta_n \ell$  :

$$\lambda_1 = 1.8751 ; \lambda_2 = 4.6941 ; \lambda_3 = 7.8547 ; \lambda_4 = 10.9955 ; \lambda_n \approx (2n-1) \frac{\pi}{2} \rightarrow \forall n > 4$$

The corresponding undamped natural frequency-angular are found by substituting the length of the beam to find each  $\beta$  and then :

$$\omega_n = \beta_n^2 \sqrt{\frac{EI}{\rho S}} \quad (7)$$



In the case of rectangular cantilever (one end clamped and the other one free), formula (8) gives the natural frequencies corresponding to the normal flexural modes of vibration of the beam (figure 4).

$$f_n = \alpha_n \frac{e}{\ell^2} \sqrt{\frac{E}{\rho}} \quad (8)$$

with  $\alpha_n = \frac{1}{4\pi\sqrt{3}} \lambda_n^2$  and  $e$  the thickness of the beam.

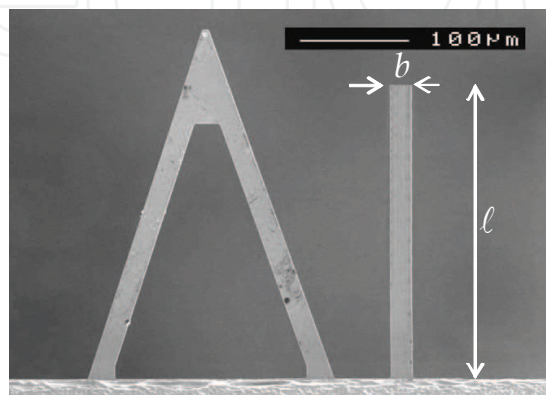


Figure 4. Description of the main geometrical parameters used in the computation

#### 4.2 Simulation with finite element method

The purpose of this analysis is to find the transient response from an harmonic load with an excitation frequency in the range 10-1000 KHz. These frequency values are typically in the range of the resonance frequencies obtained by the analytical and experimental approaches. Finite element modelling (FEM) is particularly well-suited to numerically solve the mechanical equations.

Adaptive meshing and re-meshing is used to tackle the problem of differing length scales. The 3D model makes use of an extruded triangular mesh. High-resolution solutions with minimum computation requirements are tracked. The mesh results in around 250 elements and 6000 degrees of freedom. The numerical model was defined, solved and analyzed in MATLAB using the script functions of COMSOL multiphysics (v3.4 with MEMS module) in conjunction with other in-house functions.

The FEM method was applied to two models. The first one was the three dimensional geometry (FEM 3D). The second one is a 2D Plate model where the thickness of the planar structure is less than one tenth of its width. The forces are applied in the direction normal to the plate; the main deformation takes place in the out-of-plane direction. In thin plate theory, the transverse shear deformation is neglected.

The default element type is quadratic Lagrange elements. They use second-order polynomials, which is often a good trade off between memory usage and accuracy.

In table 1, we have reported the natural frequencies obtained on a rectangular micro-cantilever. We have compared the results calculated with the formula (8), and those simulated by FEM (for the 2D Plate model and for the 3D model). As expected, a very good agreement is obtained between the three different approaches.

n	Mode	Analytic (KHz)	Plate model	FEM 3D
1	Long <sub>x</sub> 1	16.4	16.5	16.5
2	Long <sub>x</sub> 2	103,0	103.5	103.6
3	Long <sub>x</sub> 3	288.5	289.9	290.1
4	Long <sub>y</sub> 1	---	---	298.5
5	Torsional vib.	---	531.9	531.2
6	Long <sub>x</sub> 4	565.3	568.6	568.8
7	Long <sub>x</sub> 5	934.5	940.9	941.2

Table 1. Assignment of the first seven natural modes for a rectangular cantilever ( $\ell = 170 \mu\text{m}$ ,  $b = 10 \mu\text{m}$ , thickness  $e = 0,550 \mu\text{m}$ , Young's modulus: 143 GPa)

Figure 5 shows the deflection of the beam for the modes 2 and 3.

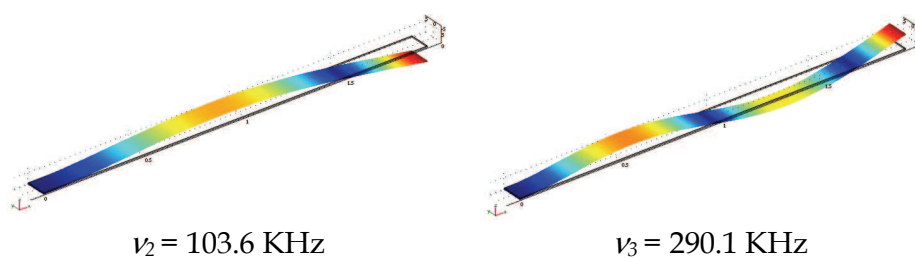


Figure 5. Deformation shapes and corresponding frequencies for two natural vibration modes:  $n=2$  and  $3$  (3D model). The boundaries display the total displacement; the black edges indicate the non-deformed beam geometry; and the white edges delineate the deformed geometry

#### 4.3 Experimental and modelling results on a rectangular beam

By using the classical detection system of an atomic force microscope, we have measured the natural frequencies of a micro-cantilever, which is generally used in intermittent contact mode. A typical spectrum is presented in figure 6. We have also reported on the graph the simulated results (blue line). For the simulation, the thickness of the beam is constituted of 430 nm of silicon and a thin film of gold (70 nm). In order to precisely mesh the structure, we have twice extruded the 2D geometry.

A good agreement is observed between experimental and calculated frequencies. However, it is interesting to note that only one parameter was adjusted in this simulation: the thickness of the thin film of gold. Indeed, an accurate knowledge of this parameter is very difficult to obtain experimentally.

This first part concerning the rectangular cantilevers is very important because it shows the ability of the COMSOL software to precisely calculate the frequencies of very thin films. Moreover, this fact is confirmed by comparing the classical analytical solutions with experimental measurements on bi-layers beams.



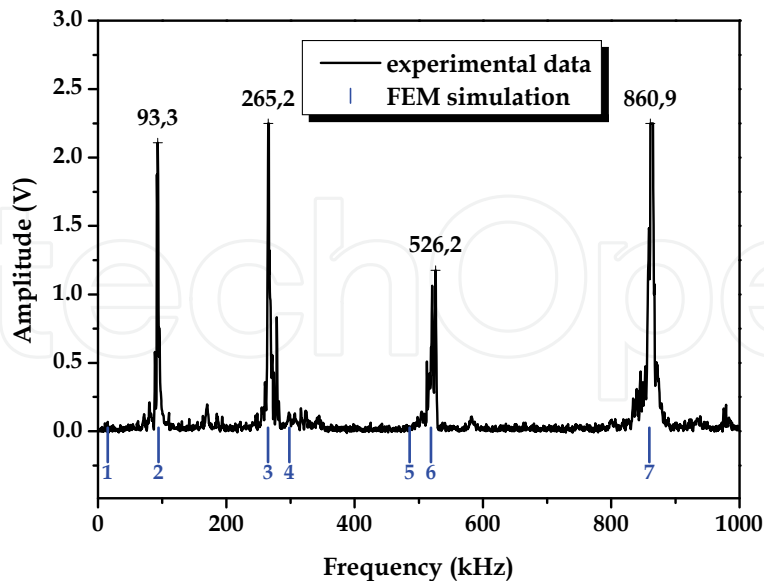


Figure 6. Experimental spectrum measured on a rectangular beam with the AFM set-up (Veeco Inst.). Underneath, we reported the FEM 3D simulated frequencies (blue line) (thickness 520 nm,  $E = 143$  GPa, density = 4,800 kg/m<sup>3</sup>, mesh: de 1,024 extruded square elements)

### 5. Natural frequencies of “V-shaped” micro-cantilevers

In the case of “V” shaped cantilevers, no exact solution (analytic resolution) is known. As an alternative approach, FEM method is particularly useful to calculate the fundamental natural frequencies. In figure 7, we present two SEM images of two commercial AFM cantilevers. The left image correspond to the STS E type and the right to the STS F type.

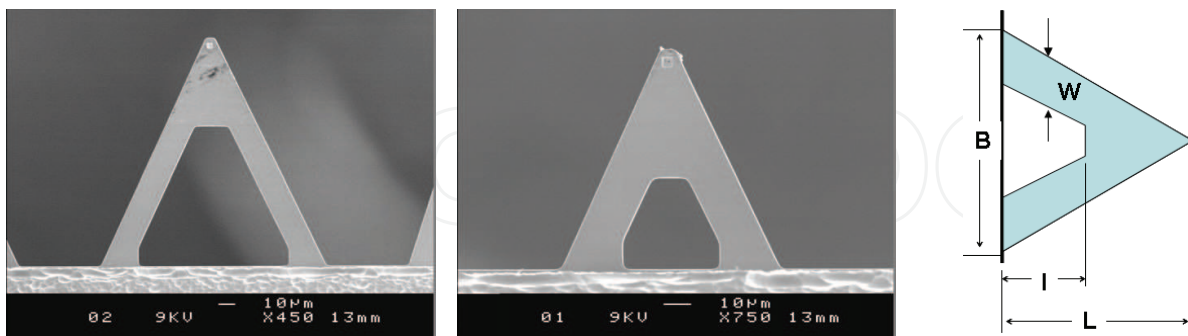


Figure 7. Examples of commercial AFM-cantilevers and definition of the main geometrical parameters used in FEM simulation.

The main geometrical parameters have been measured using SEM microscope. These parameters are defined in figure 7 and numerical values are reported in table 2. In the same way, experimental and calculated frequencies are reported in table 2.

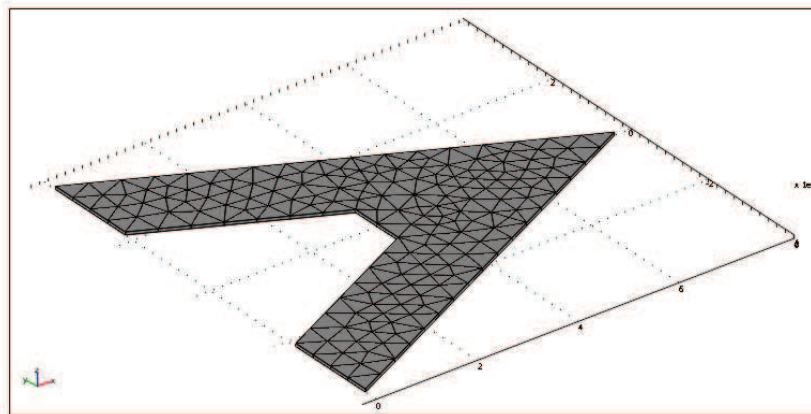


Figure 8. The 3D mesh produced by extruding a 2D triangular mesh, of very thin “V” shaped cantilever (STS F type)

A particular attention has been devoted to mesh the geometry of our cantilevers. Indeed, it is well-known that very thin structures are very difficult to simulate by FEM. Thank to the mesh module of COMSOL Multiphysics, it is possible to extrude the meshes with a very thin thickness (figure 8).

As an example, the computed deformations of the first six fundamental modes of the STS F type cantilever is presented in figure 9.

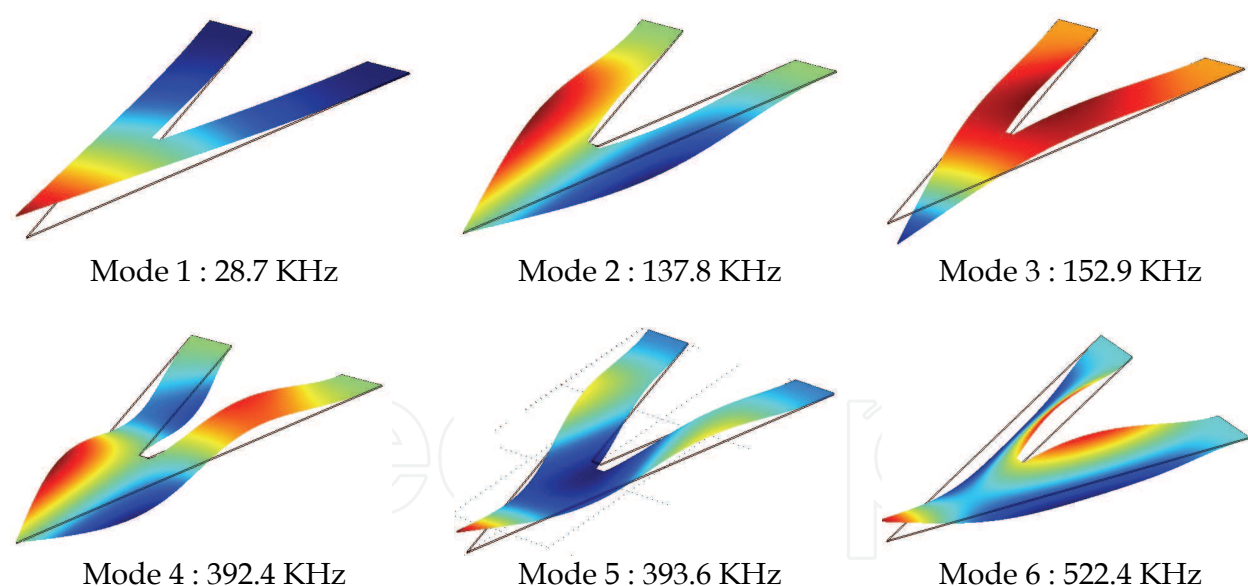


Figure 9. Deformed shapes corresponding to the first six vibration modes of the “V-shaped” cantilever. (STS F type cantilever). Underneath, FEM calculated frequencies are reported

A comparison between the natural frequencies measurements and the simulated frequencies is showed in figure 10. We have to point out that the amplitude of the first vibration mode is often very low with our experimental set-up. This amplitude is proportional to the slope of the free end of the beam but almost independent of the lateral deflection. In the simulations, the thickness of the micro-cantilever was the only adjusted parameter.

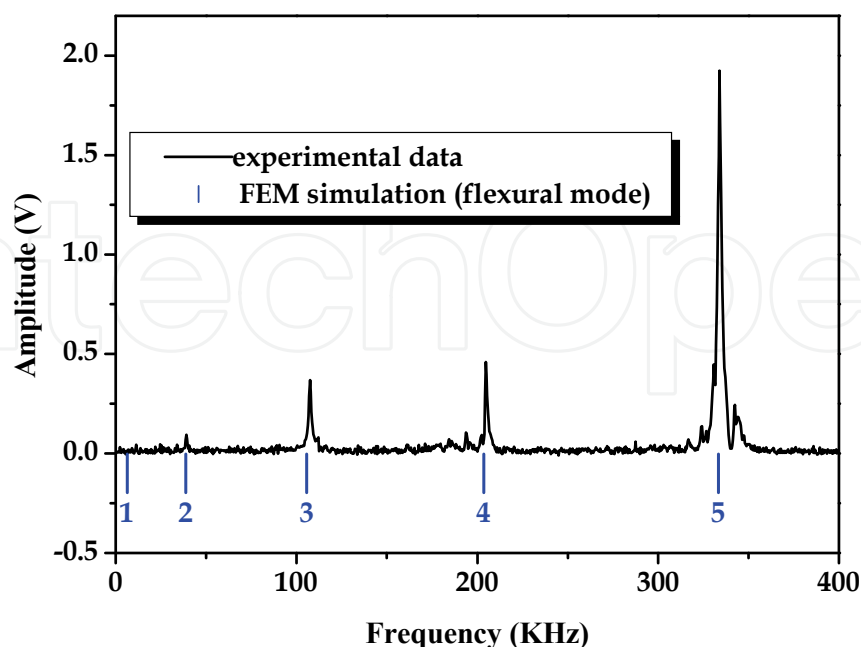


Figure 10. Experimental spectrum measured on a “V-shaped” micro-cantilever (STS C type). Underneath, the first five FEM calculated frequencies are reported

Cantilever type	L (μm)	l (μm)	w (μm)	B (μm)	Thickness (nm)	Mode n	Experimental frequency (KHz)	Simulated frequency (KHz)	Relative error (%)
STS C	323	235	21	227	680	1	-	6.41	- %
						2	39.1	38.8	0.7 %
						3	107.5	105.6	1.7 %
						4	204.6	203.6	0.4 %
						5	334.0	333.3	0.2 %
STS D	225	133	21	158	700	2	88.7	87.7	1.1 %
						3	233.2	234.4	0.5 %
STS E	128	78	18	140	560	2	193.4	194.7	0.8 %
						3	505.5	503.0	0.5 %

Table 2. Measured and simulated resonance frequencies of different “V-shaped” cantilevers (Young modulus: 143 GPa, density = 4800 kg/m<sup>3</sup>)

## 6. Natural frequencies of “V-shaped” coated cantilevers

These cantilevers can be easily coated with organic or inorganic layers, which offer interesting anchoring points for further functionalizations. For example, thin films of N,N'-diphenyl-1,4-phenylenediamine (B3) (purchased from Aldrich) were deposited on the backside of the cantilever by vacuum thermal evaporation (De Santana et al., 2006). Figure

11 presents the experimental frequency shifts of a cantilever coated with different thicknesses of B3, and the same cantilever in its uncoated state.

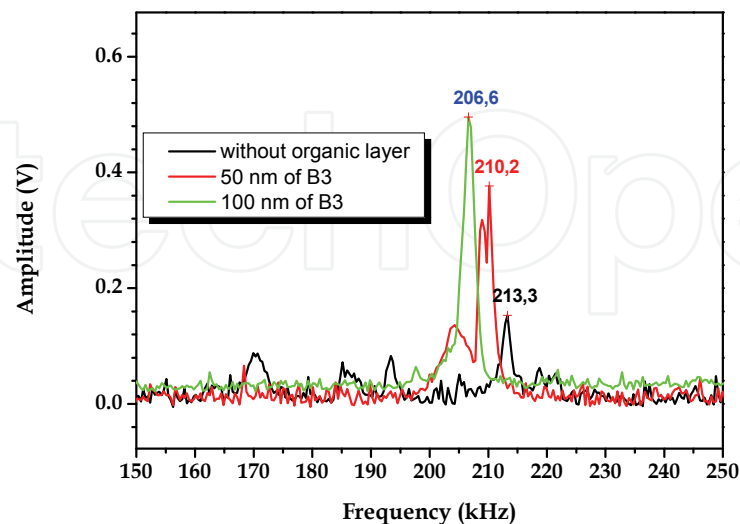


Figure 11. Resonance spectra of uncoated and organic layer - coated cantilever

By using an home-made arrangement of plasma reactors, the surface of “V-shaped” cantilevers was coated with a thin layer of platinum. Prior to the metallization, these reactors were employed to remove dust particles. Then, by plasma sputtering without breaking the vacuum, a thin layer of platinum (between 5 and 20 nm) was deposited (Chaigneau et al., 2007).

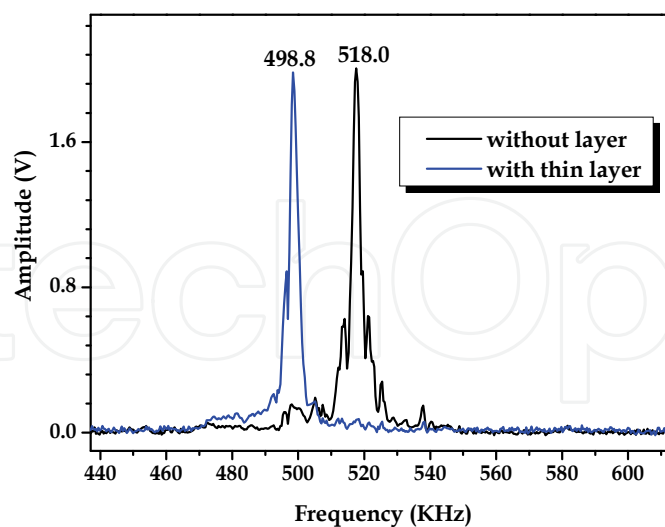


Figure 12. Resonance spectra of uncoated and platinum-coated micro-cantilever

A thin solid film of 10 nm of platinum was deposited onto a STS C type micro-cantilever. In figure 12, a significant frequency shift is observed for the coated cantilever (498.8 KHz) with respect to the frequency of the uncoated cantilever (518.0 KHz).

By taking into account the mass density and the deposited volume, a crude calculation indicates a mass change varying between 1.3 pg (platinum thickness of 5 nm) to 5.5 pg (20 nm thick).

Then, the finite element modelling can be used to evaluate the sensitivity of the used cantilever depending on the deposited thickness.

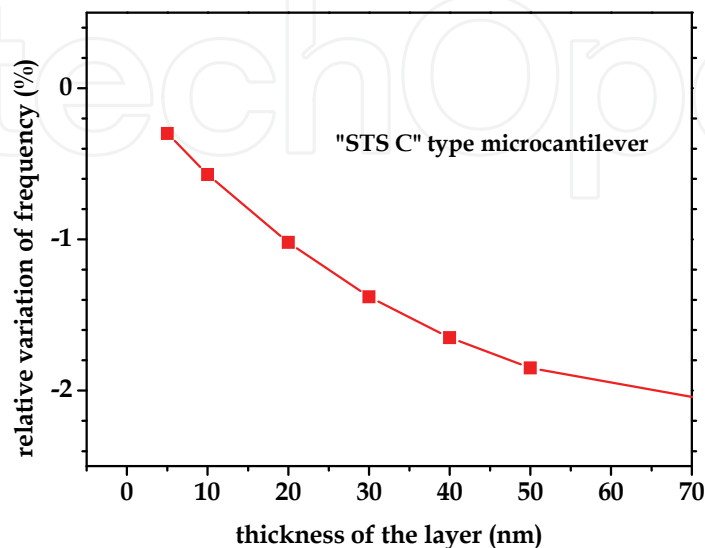


Figure 13. Relative variation of the resonance frequency as a function of the layer thickness of deposited platinum

As an example, figure 13 shows the simulated values of the frequency shift as a function of the deposited layer thickness (which can be easily converted into added mass). The slope of this curve gives us the sensitivity of the modified cantilever. In future, such simulations could be used to predict the sensitivity for different cantilevers with various geometrical dimensions, as well as for different deposited layer thicknesses.

## 7. Conclusion and prospects

The AFM cantilevers offer interesting prospects as biological and chemical sensors with very high sensitivity. To allow the adsorption of chemical species on the functionalized surface of cantilevers, these cantilevers are previously coated with a thin film of gold or silver. The sensitivity of such sensors could be predicted from the modelling of these cantilevers. As the principle of detection is generally based on the measurement of the resonance frequency shift, it seems crucial to calculate the resonance frequencies of cantilevers. For complicated shapes of cantilevers, like V-shaped cantilevers, these resonance frequencies can only be obtained by using a finite element modelling.

In this way, this chapter presents some results concerning the use of FEM to estimate the resonance frequencies of rectangular and V-shaped cantilevers. First of all, this approach was applied to rectangular micro-cantilevers to compare the analytical, experimental and FEM-computed values of the resonance frequencies. As expected, the frequencies determined by FEM approach were very close to those obtained experimentally or analytically. Then, the FEM method was employed to evaluate the frequencies of V-shaped

cantilevers, which can not be analytically calculated. By adapting the mesh parameters, a good agreement was obtained between the FEM-values and the experimental frequencies. In prospects, the same approach could be employed to predict the sensitivities of such cantilevers recovered with a sensitive layer. Moreover, an interesting use of finite element modelling would be to optimize the shape and the geometrical dimensions of these cantilevers for obtaining the best sensitivities and detection limits.

## 8. Acknowledgments

S.C. and G.L acknowledge the "Agence Nationale de la Recherche" for financial support in the frame of "ANR06-Jeunes Chercheurs-n°24" program. The authors would like to thank M. Collet for fruitful discussions.

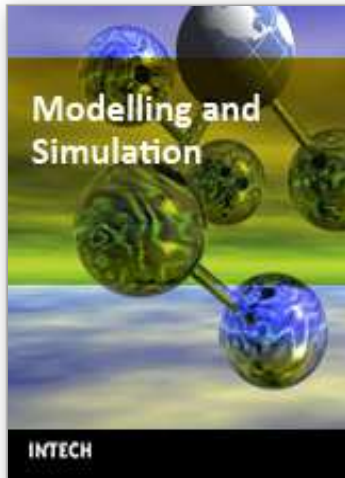
## 9. References

- Baselt, D. R.; Fruhberger, B.; Klaassen, E.; Cemalovic, S.; Britton C.L.; Patel, S. V.; Mlsna, T. E.; McCorkle, D. & Warmack, B. (2003). Design and performance of a microcantilever-based hydrogen sensor. *Sensors and Actuators B*, 88, 120-131
- Bashir, R.; Hilt, J. Z.; Elibol, O.; Gupta, A. & Peppas, N.A. (2002). Micromechanical cantilever as an ultrasensitive pH microsensor *Appl. Phys. Lett.*, 81, 3091-3093
- Betts, T. A.; Tipple, C. A.; Sepaniak, M. J. & Datskos, P. G. (2000). Selectivity of chemical sensors based on micro-cantilevers coated with thin polymer films, *Analytica Chimica Acta*, 422, 89 -99
- Chaigneau, M.; Minea, M. & Louarn, G. (2007). Comparative study of different process-steps for the near-field optical probes manufacturing. *Ultramicroscopy* 107 1042-1047
- Chen, G. Y.; Thundat, T., Wachter, E. A. & Warmack, R. J. (1995). Adsorption-induced surface stress and its effects on resonance frequency of microcantilevers *J. Appl. Phys.* 77(8), 3618-3622
- Cuenot, S.; Fretigny, C.; Demoustier-Champagne, S. & Nysten B. (2003). Measurement of elastic modulus of nanotubes by resonant contact atomic force microscopy *J. Appl. Phys.* 93, 5650 (2003).
- De Santana, H.; Quillard, S.; Fayad, E. & Louarn, G. (2006). In situ UV-VIS and Raman spectroscopic Studies of the electrochemical behavior of N,N'-Diphenyl-1,4-Phenylenediamine. *Synthetic Metals* 156 81-85
- Dufour, I. & Fadel, L. (2003). Resonant microcantilever type chemical sensors: Analytical modelling in view of optimization. *Sensors and Actuators B*, 91, 353-361
- Gimzewski, J. K.; Gerber, C., Meyer, E. & Schlittler, R. R. (1994). Observation of a chemical reaction using a micromechanical sensor *Chem. Phys. Let.* 217, 589-594
- Ji, H- F.; Hansen, K. M.; Hu, Z. & Thundat, T. (2001). Detection of pH variation using modified microcantilever sensors *Sensors and Actuators B* 72, 233-238
- Lange, D.; Hagleitner, C.; Hierlemann, A.; Brand, O. & Baltes, H. (2002). Complementary metal oxide semiconductor cantilever arrays on a single chip: Mass-sensitive detection of volatile organic compounds. *Analytical Chemistry*, 74, 3084 -3095
- Lavrik N.; Sepaniak M. & Datskos P. (2004). Cantilever transducers as a platform for chemical and biological sensors. *Rev. Sci. Instrum.*, 75, 2229-2253



- Lochon, F.; Dufour, I. & Rebière, D. (2005). An alternative solution to improve sensitivity of resonant microcantilever chemical sensors: Comparison between using high-order modes and reducing dimensions. *Sensors and Actuators B*, 108, 979-985
- Moulin, A. M.; O'Shea, S. J. & Welland, M.E. (2000). Microcantilever-based biosensors *Ultramicroscopy* 82, 23-31
- Raiteri, R.; Grattarola, M.; Butt, H. -J. & Skládal, P. (2001). Micromechanical cantilever-based biosensors. *Sensors and Actuators B*, 79, 115-126
- Sepaniak, M.; Datskos, P.; Lavrik, N. & Tipple, C. (2002). Microcantilever transducers: A new approach in sensor technology. *Analytical Chemistry*, 74, 568 -575
- Stokey W. F. (1988). Vibration of systems having distributed mass and elasticity, In: *Shock and vibration Handbook*, Cyril M. Harris (Ed.), chapter 7, McGraw Hill book Company, ISBN 0-07-026801-0, New-York, USA
- Thundat, T.; Wachter, E. A.; Sharp, S.L. & Warmack, R. J. (1995a). Detection of mercury vapor using resonating microcantilevers. *Appl. Phys. Lett.*, 66, 1695-1697
- Thundat, T.; Sharp, S. L.; Fisher, W. G.; Warmack, R. J. & Wachter E. A. (1995b). Micromechanical radiation dosimeter *Appl. Phys. Lett.* 66, 1563-1565
- Wachter, E. A. & Thundat, T. (1995). Micromechanical sensors for chemical and physical measurements. *Rev. Sci. Instrum.*, 66, 3662-3667

IntechOpen



## **Modelling and Simulation**

Edited by Giuseppe Petrone and Giuliano Cammarata

ISBN 978-3-902613-25-7

Hard cover, 688 pages

**Publisher** I-Tech Education and Publishing

**Published online** 01, June, 2008

**Published in print edition** June, 2008

This book collects original and innovative research studies concerning modeling and simulation of physical systems in a very wide range of applications, encompassing micro-electro-mechanical systems, measurement instrumentations, catalytic reactors, biomechanical applications, biological and chemical sensors, magnetosensitive materials, silicon photonic devices, electronic devices, optical fibers, electro-microfluidic systems, composite materials, fuel cells, indoor air-conditioning systems, active magnetic levitation systems and more. Some of the most recent numerical techniques, as well as some of the software among the most accurate and sophisticated in treating complex systems, are applied in order to exhaustively contribute in knowledge advances.

### **How to reference**

In order to correctly reference this scholarly work, feel free to copy and paste the following:

G. Louarn and S. Cuenot (2008). Finite Element Modelling of Micro-cantilevers Used as Chemical Sensors, Modelling and Simulation, Giuseppe Petrone and Giuliano Cammarata (Ed.), ISBN: 978-3-902613-25-7, InTech, Available from:

[http://www.intechopen.com/books/modelling\\_and\\_simulation/finite\\_element\\_modelling\\_of\\_micro-cantilevers\\_used\\_as\\_chemical\\_sensors](http://www.intechopen.com/books/modelling_and_simulation/finite_element_modelling_of_micro-cantilevers_used_as_chemical_sensors)

**INTECH**  
open science | open minds

### **InTech Europe**

University Campus STeP Ri  
Slavka Krautzeka 83/A  
51000 Rijeka, Croatia  
Phone: +385 (51) 770 447  
Fax: +385 (51) 686 166  
[www.intechopen.com](http://www.intechopen.com)

### **InTech China**

Unit 405, Office Block, Hotel Equatorial Shanghai  
No.65, Yan An Road (West), Shanghai, 200040, China  
中国上海市延安西路65号上海国际贵都大饭店办公楼405单元  
Phone: +86-21-62489820  
Fax: +86-21-62489821

© 2008 The Author(s). Licensee IntechOpen. This chapter is distributed under the terms of the [Creative Commons Attribution-NonCommercial-ShareAlike-3.0 License](#), which permits use, distribution and reproduction for non-commercial purposes, provided the original is properly cited and derivative works building on this content are distributed under the same license.

IntechOpen

IntechOpen